RESEARCH

Reliability of wing morphometrics for species identification of human-biting black flies (Diptera: Simuliidae) in Thailand

Kittipat Aupalee[1], Wichai Srisuka[2], Kwankamol Limsopatham[1], Sangob Sanit[1], Hiroyuki Takaoka[3] and Atiporn Saeung[1*]

Abstract

Background Fast and reliable species identification of black flies is essential for research proposes and effective vector control. Besides traditional identification based on morphology, which is usually supplemented with molecular methods, geometric morphometrics (GM) has emerged as a promising tool for identification. Despite its potential, no specific GM techniques have been established for the identification of black fly species.

Methods Adult female black flies collected using human bait, as well as those reared from pupae, were used in this study. Here, landmark-based GM analysis of wings was assessed for the first time to identify human-biting black fly species in Thailand, comparing this approach with the standard morphological identification method and DNA barcoding based on the mitochondrial cytochrome *c* oxidase subunit I (*COI*) gene. To explore genetic relationships between species, maximum likelihood (ML) and neighbor-joining (NJ) phylogenetic trees were built. Additionally, three different methods of species delimitation, i.e., assemble species by automatic partitioning (ASAP), generalized mixed yule coalescent (GMYC), and single Poisson tree processes (PTP), were utilized to identify the morphologically defined species. The effectiveness of a *COI* barcode in identifying black fly species was further examined through the best match (BM) and best close match (BCM) methods.

Results Seven black fly species, namely *Simulium tenebrosum* Takaoka, Srisuka & Saeung, 2018 (complex), *S. doipuiense* Takaoka & Choochote, 2005 (complex), *S. nigrogilvum* Summers, 1911, *S. nodosum* Puri, 1933, *S. asakoae* Takaoka & Davies, 1995, *S. chamlongi* Takaoka & Suzuki, 1984, and *S. umphangense* Takaoka, Srisuka & Saeung, 2017 were morphologically identified. Compared with the standard method, the GM analysis based on wing shape showed high success in separating species, achieving an overall accuracy rate of 88.54%. On the other hand, DNA barcoding surpassed wing GM for species identification with a correct identification rate of 98.57%. Species delimitation analyses confirmed the validity of most nominal species, with an exception for *S. tenebrosum* complex and *S. doipuiense* complex, being delimited as a single species. Moreover, the analyses unveiled hidden diversity within *S. asakoae*, indicating the possible existence of up to four putative species.

Conclusions This study highlights the potential of wing GM as a promising and reliable complementary tool for species identification of human-biting black flies in Thailand.

Keywords Morphometric analysis, DNA barcodes, Species delimitation, Hematophagous insect, Medical entomology, *Simulium*

*Correspondence:
Atiporn Saeung
atisaeung.noi@gmail.com
Full list of author information is available at the end of the article

Aupalee *et al. Parasites & Vectors*   (2024) 17:508

Page 2 of 17

Background

Black flies are small, dark, humpbacked flies that belong to the family Simuliidae, with more than 2400 species formally recorded worldwide [1]. The female flies usually feed on the blood of birds and mammals, including humans, which can cause irritation, pain, swelling, and redness at the bite site due to an immunoglobulin (Ig) E-mediated reaction to salivary gland proteins [2–9]. During the biting, some species could transmit various pathogens to both animals and humans, especially the filarial worm *Onchocerca volvulus*, the causative agent of human onchocerciasis or river blindness [9, 10]. This disease is the second leading cause of infectious blindness globally and is one of the 21 neglected tropical diseases (NTDs) that the World Health Organization (WHO) has targeted for elimination by 2030 [11]. In Thailand, a total of 146 species of black flies have been officially documented, with seven species (*Simulium asakoae*, *S. nigrogilvum*, *S. tenebrosum* complex, *S. doipuiense* complex, *S. umphangense*, *S. chamlongi*, and *S. nodosum*) considered to be human biters [12–15]. Most recently, host blood meal analysis of adult flies based on mitochondrial cytochrome *b* (*cytb*) gene revealed that two other species, *S. chumpornense* Takaoka & Kuvangkadilok, 2000 and *S. striatum* species-group fed on human blood [16]. However, no human infectious diseases transmitted by these flies have been reported so far in the country [17]. Notably, three human-biting species, namely *S. asakoae*, *S. nigrogilvum* and *S. nodosum*, have been incriminated as natural vectors of various species of filarial or nonfilarial worms, including the genus *Onchocerca* [17–22]. Furthermore, *S. chumpornense*, *S. khelangense* Takaoka, Srisuka & Saeung, 2022, and *S. asakoae* were recently identified as natural vectors of avian blood protozoa of the genera *Leucocytozoon* and *Trypanosoma* [23–26]. Considering the critical role of black flies as vectors for transmitting diverse pathogens, rapid and accurate species identification is crucial for comprehending disease epidemiology and developing effective vector control measures [27].

Traditionally, black fly species identification relies on meticulous examination of morphological characteristics of a large series of larvae, pupae, and adults (males and females), sometimes even requiring dissection [28]. Due to the small size and morphological uniformity of this insect, morphological classification is extremely difficult and often requires trained experts, proving impractical or even impossible for specimens that are damaged or closely related species [28, 29]. To overcome these limitations, other methods (cytogenetics and DNA barcoding) have been developed and used together to assist black fly species identification and confirmation [29–32]. Currently, DNA barcoding based on *COI* gene sequences plays a significant role in black fly species identification, enabling researchers to distinguish species rapidly and accurately. This method is not only used as an effective identification tool, but can also reveal hidden diversity within nominal species [28, 33–39]. Nevertheless, molecular approaches are relatively expensive, sophisticated, and need to be conducted in well-equipped laboratories [40, 41]. A faster, cost-effective, easy to use, and reliable method for accurately identifying species is necessary.

Over the past decade, geometric morphometrics (GM) analysis has emerged as a potential game changer, being used as an effective complementary tool for the species identification of various insect groups, particularly those with medical and veterinary importance [41–50]. This approach has also proved to be a valuable tool for detecting sexual dimorphism, recognition of cryptic diversity, and studying evolution [48, 51–55]. Presently, the landmark-based GM method of insect wings is the most popular and is a powerful tool used for supplementing and enhancing morphological identification [56, 57]. This method analyzes wing size and shape based on the positions of anatomical landmarks (also known as true landmarks) and the distances between them, which includes both size and shape data [56, 57]. While GM analysis has been employed successfully for distinguishing species of several insect groups, its application for black fly identification remains unexplored. To the best of our knowledge, there is only one study that applied this technique for interpreting evolutionary transitions in the black fly wings [51].

In the present study, landmark-based GM analysis of wings was evaluated, for the first time, for the identification of seven human-biting black fly species of Thailand. For comparison, DNA barcoding based on the *COI* gene was used to distinguish the species and the effectiveness of this gene for species identification was also tested using the best match (BM) and best close match (BCM) methods. Additionally, three species delimitation methods [assemble species by automatic partitioning (ASAP), generalized mixed yule coalescent (GMYC), and single Poisson tree processes (PTP)] were employed to identify the recognized morphospecies.

Methods

Black fly samples and morphological identification

Most adult female flies were caught with a sweep net while flying around a human bait, while others were reared from pupae collected with fine forceps from available substrates in streams. The wild-caught females were promptly euthanized by submerging them in a 15 ml centrifuge tube containing 80% alcohol. Meanwhile, matured pupae were kept individually in a 15 ml centrifuge tube with minimal water at the bottom until adulthood. The

Aupalee *et al. Parasites & Vectors* (2024) 17:508

Page 3 of 17

emerged adult females were kept alive in the same tube for at least 24 h to ensure the hardening and coloration of their exoskeleton [15]. All specimens were preserved in 80% ethanol and stored in a freezer (−20 °C) until further analysis. Species identification of the adult flies was based on the examination of their morphological characteristics under a stereomicroscope (Olympus SZ51, Japan) using the standard keys for the black flies of Thailand [58]. In total, 253 adult female black flies (seven species or complex) belonging to the subgenera *Gomphostilbia* [one species designated here as "*S. asakoae*" although our specimens probably include not only *S. asakoae* but also several other species of the *S. asakoae* species-group, which are morphologically indistinguishable from one another (*n* = 50)] and *Simulium* s. str. [six species including *S. chamlongi* (*n* = 30), *S. doipuiense* complex (*n* = 39), *S. nigrogilvum* (*n* = 39), *S. nodosum* (*n* = 31), *S. tenebrosum* complex (*n* = 31), and *S. umphangense* (*n* = 33)] of the genus *Simulium* Latreille s. l. were utilized in this study as outlined in Table 1.

Wing preparation, image processing, and landmark digitization

After morphological identification of the species, at least 30 specimens of each black fly species with intact wings were selected for geometric morphometric analysis

(Table 1). A subset of these fly samples (ten specimens/species) was also randomly chosen for molecular analysis.

To prepare a semi-permanent slide, the right wing of each individual was first removed from the thorax using an insect needle under a stereomicroscope (Olympus SZ51, Japan). Each wing was then transferred to a new slide, placed on a drop of 80% alcohol, and covered with a coverslip. To prevent leakage and evaporation of the alcohol while observing and photographing the specimens, air-drying nail polish (Revlon, Indonesia) was applied to seal the edges of a coverslip. Digital images of each wing were captured using a DP27 digital camera attached to a 4× magnification light microscope (Olympus CX41, Japan). All images were annotated with a 500 µm reference scale bar. A total of ten landmarks (Fig. 1) slightly modified from [51] were digitized on each wing.

Repeatability
To assess the accuracy of digitizing landmarks, a repeatability test for the shape was performed. Ten wing images of each fly species were randomly selected and digitized twice by the same user for intra-user repeatability. The measurement error, expressed as the repeatability index (*R*), was calculated by comparing two sets of digitized images using the Procrustes analysis of variance (ANOVA) method [59].

Table 1 Details of adult female black flies used in this study

Species	Sampling site	Coordinate (latitude/longitude)	Elevation (m)	Date of collection	*n*	Total
S. asakoae	Ban Pang Dang, Doi Saket, Chiang Mai	19°03′35.0″ N/99°21′52.9″ E	932	28 August 2023	25	50
	Ban Pang Bong, Doi Saket, Chiang Mai	18°49′04.3″ N/99°20′06.2″ E	981	28 August 2023	25	
S. chamlongi	A-Frame, Doi Pha Hom Pok, Chiang Mai	20°02′12.9″ N/99°09′55.8″ E	1529	29 November 2012	21[a]	30
	Mae Kam Pong Waterfall, Mae On, Chiang Mai	18°51′48.6″ N/99°21′22.9″ E	1076	1 June 2015	4[a]	
	Pangkhon, Mueang, Chiang Rai	19°54′17.6″ N/99°35′54.0″ E	1386	29 October 2016	5[a]	
S. doipuiense complex	Mae Klong Kee, Umphang, Tak	16°13′33.0″ N/98°58′46.8″ E	1264	24 June 2021	2	39
	Mae Klong Kee Unit, Umphang, Tak	16°14′45.8″ N/98°59′52.1″ E	1188	17 August 2021	12	
		16°13′30.9″ N/98°58′47.3″ E	1237	18 August 2021	16	
	Pa Deuk Dum Bun, Umphang, Tak	16°14′38.0″ N/98°59′55.6″ E	1263	19 August 2021	9	
S. nigrogilvum	Mae Klong Kee, Umphang, Tak	16°13′29.1″ N/98°58′44.9″ E	1279	24 June 2021	12	39
	Mae Klong Kee Unit, Umphang, Tak	16°14′45.8″ N/98°59′52.1″ E	1188	17 August 2021	19	
		16°13′30.9″ N/98°58′47.3″ E	1237	18 August 2021	8	
S. nodosum	Tham Pla, Mueang, Mae Hong Son	19°30′09.2″ N/98°00′22.9″ E	385	24 October 2014	20	31
	Tao Dam Waterfall, Khlonglan, Kamphaeng Phet	16°18′04.6″ N/99°06′44.3″ E	539	20 December 2016	11[a]	
S. tenebrosum complex	Doi Inthanon, Chom Thong, Chiang Mai	18°35′12.8″ N/98°29′14.2″ E	2534	19 December 2018	31	31
S. umphangense	Ban Lek, Doi Pha Hom Pok, Chiang Mai	20°04′30.9″ N/99°11′07.4″ E	1468	29 May 2010	1	33
	Chong Yen, Mae Wong, Kamphaeng Phet	16°06′02.3″ N/99°06′29.0″ E	1276	23 March 2016	3	
				19 January 2017	13	
				4 November 2018	3	
	Mae Klong Kee Unit, Umphang, Tak	16°13′34.8″ N/98°58′46.1″ E	1272	1 March 2013	6	
	Upstream Mae Klong Yai, Umphang, Tak	16°18′00.5″ N/99°01′22.6″ E	1095	22 March 2016	1	
	Pa Deuk Dum Bun, Umphang, Tak	16°14′38.0″ N/98°59′55.6″ E	1263	5 March 2020	3	
	Mae Klong Kee, Umphang, Tak	16°13′33.0″ N/98°58′46.8″ E	1264	24 June 2021	3	

[a] Adult female reared from pupa

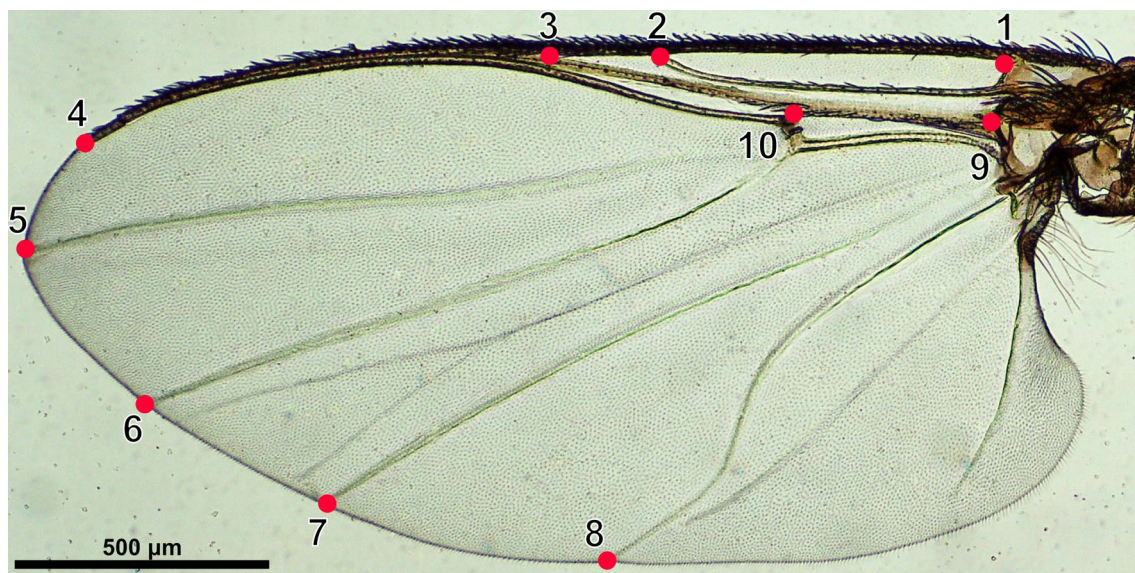Aupalee *et al. Parasites & Vectors*   (2024) 17:508

Page 4 of 17

Fig. 1 A representative image of black fly wing showing ten landmarks used in geometric morphometric analysis

Allometry

As previously reported, wing sizes could influence wing shape variation (allometry) [60, 61]. This correlation was examined before conducting the wing shape analysis. The coefficient of determination (R^2), obtained from analyzing the linear regression between the wing centroid size (CS) and the first principal component (PC) of wing shape, was used to assess the extent of the influence.

Wing size and shape analysis

To estimate the global wing size of each species, we employed the centroid size (CS), which was derived from the distances between the centroid point of each configuration and each landmark [62]. The variation of wing CS among *Simulium* species was illustrated using a violin plot. Statistically significant differences in wing CS between species were assessed using a one-way ANOVA (1000 iterations) with Bonferroni adjustment for significance testing at a p-value < 0.05.

For the wing shape analysis, shape variables were derived through a Procrustes superimposition of landmark configurations using the generalized Procrustes analysis (GPA) [63, 64]. Subsequently, partial wrap scores generated from principal component analysis were used as final shape variables for subsequent analyses. To explore species separation, discriminant analysis (DA) was performed using the final shape variables as an input and was illustrated as a factor map. The Mahalanobis distance, obtained from DA analysis, was calculated to estimate shape divergence between species. Wing shape differences among species based on the Mahalanobis distances were analyzed using a nonparametric permutation test (1000 iterations) with a Bonferroni adjustment for significance testing at a p-value < 0.05. Additionally, a hierarchical clustering tree (UPGMA algorithm) based on Mahalanobis distances was constructed to assess the relationships of wing shape among species [65].

Validated classification

A cross-validated classification (jackknife classification) was performed to test the accuracy of wing size and shape for correct species identification [66]. Each individual was successively excluded from the total sample and then allocated to the most probable group for size and the nearest group for shape using the maximum likelihood method [67] and Mahalanobis distance [68], respectively.

Morphometric software

The geometric morphometrics analysis, including landmark digitization, repeatability test, allometric examination, wing size and shape analyses, and a cross-validated classification test were performed using the online application XY Online Morphometrics (XYOM) version 2 [69]. The software is freely accessible at https://xyom.io/, accessed on 10 March 2024. In addition, the results generated from the XYOM were further beautified in RStudio [70].

Molecular identification based on DNA barcoding

For supplementing the morphological species identification, DNA barcoding using the *COI* gene was performed on the randomly selected specimens of each black fly species (ten specimens/species). Total DNA was

Aupalee *et al. Parasites & Vectors*   (2024) 17:508

Page 5 of 17

extracted from the thorax of individual flies using the TIANamp Genomic DNA Kit (TIANGEN Biotech, Beijing, China), according to the manufacturer's protocol. A DNA fragment of the mitochondrial *COI* gene (658 bp in length) was amplified using the universal primers: LCO1490 (5′-GGT CAA CAA ATC ATA AAG ATA TTG G-3′) and HCO2198 (5′-TAA ACT TCA GGG TGA CCA AAA AAT CA-3′) [71]. Each PCR reaction (20 μl total volume) was composed of 2 μl of DNA template, 1 U of Taq DNA polymerase, 3 mM $MgCl_2$, 0.2 mM dNTPs, and 0.2 μM of each primer. The PCR cycling conditions included: an initial denaturation at 94 °C for 2 min followed by 40 cycles at 94 °C for 30 s, 50 °C for 45 s, and 72 °C for 45 s, with a final extension at 72 °C for 5 min. Subsequently, the PCR products were checked by agarose gel electrophoresis (1.5%), visualized by non-toxic Ultrapower (BioTeke, Beijing, China) dye. All PCR samples with a band of the expected size (658 bp) were sent to First Base Laboratories Sdn Bhd (Malaysia) for purifying and sequencing using the BigDye Terminator v.3.1 cycle sequencing kit on an ABI 3730XL Genetic Analyzer (Applied Biosystems Inc., Foster City, CA, USA). To generate a consensus sequence of each specimen, both forward and reverse sequences were assembled and edited manually in Geneious Prime 2024.0.5 [72]. Calculation of intra- and interspecific genetic distances based on the Kimura two-parameter (K2P) model [73] was conducted in MEGA 11 [74, 75]. The species identities of each black fly specimen were determined by comparing the newly generated sequences with previously published sequences deposited in the GenBank database, using the basic local alignment search tool (BLAST), available at http://blast.ncbi.nlm.nih.gov/Blast.cgi. Success rates of the DNA barcoding in species identification were evaluated based on the BM and BCM methods using the TaxonDNA [76]. All *COI* sequences obtained in the present study were deposited in the GenBank database under the following accession numbers: PP422429–PP422472.

Multiple sequence alignment and phylogenetic analysis
All sequences obtained in this study and others fetched from GenBank database were aligned with MUSCLE 3.7 [77], performed in MEGA 11 [74, 75]. Subsequently, the *COI* alignment was used to infer the genetic relationships among seven human-biting black fly species based on the neighbor-joining (NJ) and maximum likelihood (ML) methods. The NJ tree was constructed in MEGA 11 based on the K2P model with 1000 bootstrap iterations [74, 75, 78], while the ML tree was reconstructed using IQ-TREE version 2.3.1 [79] with 10,000 ultrafast bootstrap iterations [80]. The best-fitting substitution model for the ML method, which was K3Pu+F+I+R2, was selected using ModelFinder based on Bayesian Information Criterion

(BIC) [81]. The final tree, visualized by FigTree version 1.4.4 (http://tree.bio.ed.ac.uk/software/figtree/), was rooted using the *COI* sequence of *S. khongchiamense* Takaoka, Srisuka & Saeung, 2023, a member of the subgenus *Asiosimulium*.

Species delimitation analysis
Three different methods of DNA sequence-based species delimitation, including ASAP, GMYC, and single PTP were performed to estimate the number of molecular operational taxonomic units (MOTUs). ASAP, a distance-based method, was conducted online using the ASAP webserver, available at https://bioinfo.mnhn.fr/abi/ public/asap/, with default parameters [82]. The PTP analysis was run through mPTP webserver (https://mptp.h-its.org/#/tree) using the maximum likelihood implementation with a single Poisson distribution [83]. The ML tree generated from IQ-TREE was used as the input tree in the PTP analysis with a default *p*-value of 0.001. For the GMYC analysis, an ultrametric tree was generated with BEAUti2 software under the Yule process speciation model and the relaxed clock log-normal model [84, 85]. The best fitting substitution model (TrN+I+G) based on the BIC was determined using jModelTest 2.1.7 [86]. The MCMC chain was run in BEAST v2.6.7 for 20 million iterations with sampling frequency of 1000 iterations each. As previously recommended [87], the output file was checked using Tracer v1.7 software to ensure that all the effective sample size (ESS) values were greater than 200. To infer a maximum clade credibility tree from the set of posterior trees, the output tree was subjected to TreeAnnotator v2.6.7 with a burn-in of 20% [85]. The resulting tree was then analyzed under the single-threshold operation using the R package "splits" on the R platform [70, 88].

Results
Repeatability
The repeatability test for the wing shape revealed a very low measurement error score (1%) and a high repeatability score (99%), suggesting a high level of accuracy in landmark placement on the tested wing image set.

Allometric effect
Assessment of the allometric effect revealed an apparent negative relationship between wing size and wing shape ($R^2 = 33.7\%$) with statistical significance ($p < 0.05$) (Fig. 2). This indicated that wing size variation influences wing shape divergence between species.

Wing size variation
The variation in wing size (CS) among seven human-biting black fly species is depicted in Fig. 3.
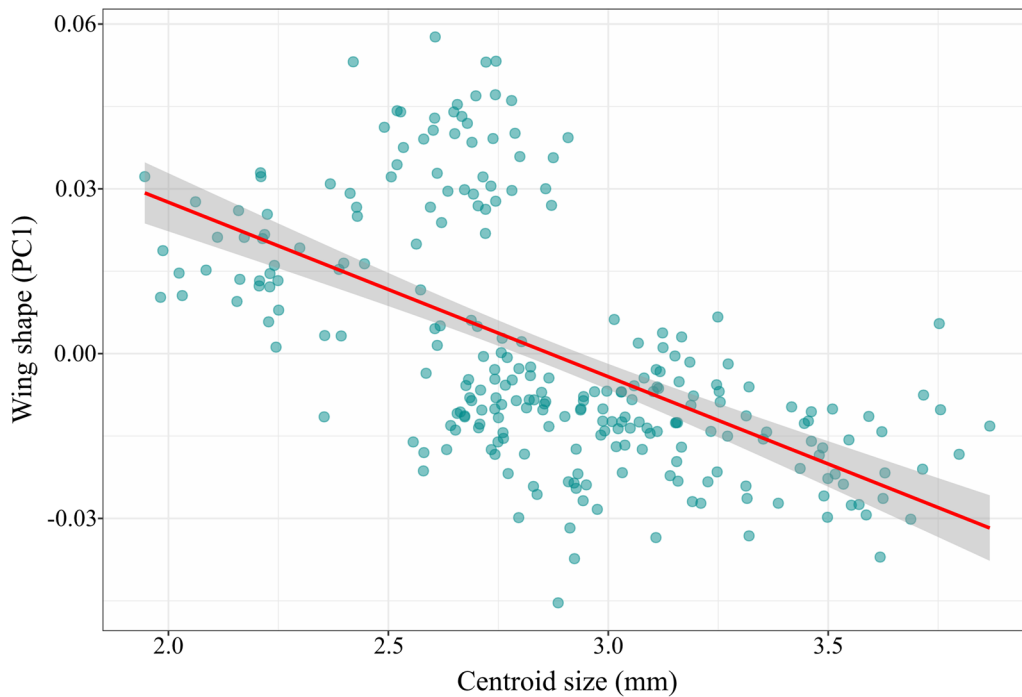
Fig. 2 Scatter plot showing the allometric relationship between the wing shape (the first principal component, PC1) and wing size (centroid size) of seven black fly species. The red line indicates the linear regression prediction with 95% confidence intervals (shaded areas), while the sapphire dots represent individual samples
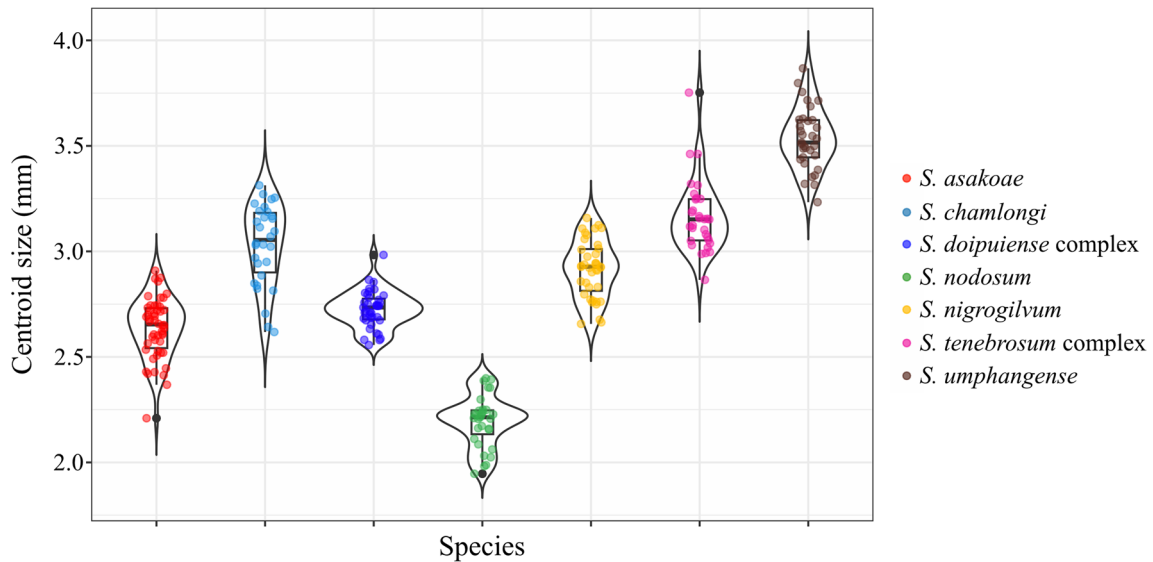

- S. asakoae
- S. chamlongi
- S. doipuiense complex
- S. nodosum
- S. nigrogilvum
- S. tenebrosum complex
- S. umphangense

Fig. 3 Violin plot overlaid with a box plot showing the distribution of wing centroid sizes (CS) in millimeters (mm) of seven black fly species

Simulium umphangense displayed the largest wing size of 3.53 ± 0.15 mm (mean ± S.D.), while *S. nodosum* exhibited the smallest wing size at 2.19 ± 0.12 mm (Table 2). The comparisons of wing size based on a nonparametric permutation test (1000 iterations) with Bonferroni adjustment revealed significant differences ($p < 0.05$) between almost all species pairs, with the exception of *S. asakoae* versus *S. doipuiense* complex and *S. chamlongi* versus *S. nigrogilvum* and *S. tenobrosum* complex.

Aupalee *et al. Parasites & Vectors*   (2024) 17:508

Page 7 of 17

Table 2 Average wing centroid sizes (CS) in millimeters and statistical differences in wing size among seven human-biting black fly species

Species	n	Wing size (mm)		
		Mean ± SD	Minimum	Maximum
S. asakoae	50	2.64 ± 0.14[a]	2.21	2.91
S. chamlongi	30	3.03 ± 0.19[b]	2.62	3.31
S. doipuiense complex	39	2.72 ± 0.09[a]	2.56	2.98
S. nodosum	31	2.19 ± 0.12[c]	1.95	2.40
S. nigrogilvum	39	2.92 ± 0.14[b,d]	2.66	3.16
S. tenebrosum complex	31	3.17 ± 0.17[b,e]	2.86	3.75
S. umphangense	33	3.53 ± 0.15[f]	3.23	3.87

Different superscript letters denote statistically significant differences at $p < 0.05$

Wing shape variation

The visual comparisons of superimposition of the mean landmark configurations among seven black fly species showed the most noticeable landmark displacement in the lower part of the wing, particularly in landmark positions 3 and 4 (Fig. 4). The analysis also indicated that *S. asakoae* exhibited the most different wing shape, as its landmark position 4 clearly separated it from the other six species (Fig. 4).

Discriminant analysis of the wing shape variables among the seven black fly species showed clear separation, with a small overlap for two species, namely *S. asakoae* and *S. nodosum*. Conversely, the five other species revealed large overlapping among species, especially the two closely related species complexes, *S.*
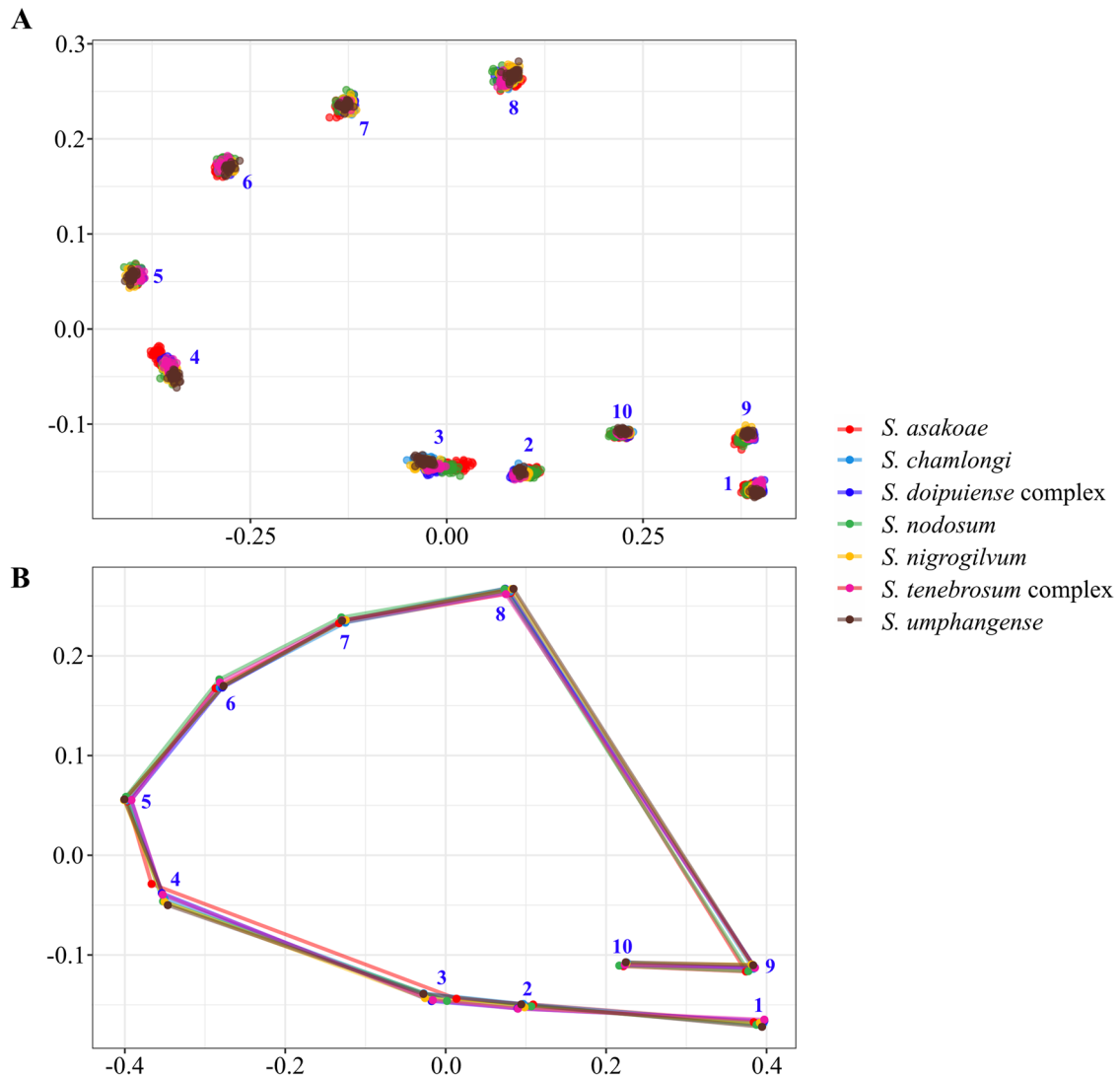

Fig. 4 Shape differences in wing venation based on anatomical landmarks of seven black fly species. (**A**) Scatter plot showing residual coordinates of ten landmarks aligned by Procrustes analysis and (**B**) a wireframe graph showing the superposition of the overall mean shape

tenebrosum complex and *S. doipuiense* complex (Fig. 5). Despite the large overlap among species, significant differences ($p < 0.05$) in wing shape were observed among all black fly species based on the pairwise Mahalanobis distances (Table 3).

Phenetic relationships of wing shape among black fly species

The UPGMA dendrogram based on Mahalanobis distances demonstrated that the seven black fly species were separated into two distinct groups (Fig. 6). *Simulium nodosum* and *S. asakoae* formed one group, while the other five species formed another group, which was further divided into two subgroups: (1) *S. chamlongi* + (*S. umphangense* + *S. nigrogilvum*) and (2) *S. tenebrosum* complex + *S. doipuiense* complex.

Validated classification

The success rate of landmark-based GM analysis of the wings for identifying seven black fly species is summarized in Tables 4 and 5. The size-based cross-validated classification revealed a low level of correct identification, with an overall accuracy score of 47.43% (120/253), while the shape-based cross-validated classification yielded a higher level of successful identification, with a total classification score of 88.54% (224/253). Furthermore, the shape-based classification showed a perfect result (100% accuracy score) for species identification of *S. asakoae*.

Sequence variation and genetic distance

In total, 70 *COI* sequences (658 bp long) of seven human-biting black fly species were obtained in this study, with 44 sequences identified as unique haplotypes. Sequence analysis revealed a high AT content, with an average base composition of A = 0.275, C = 0.178, G = 0.168, and
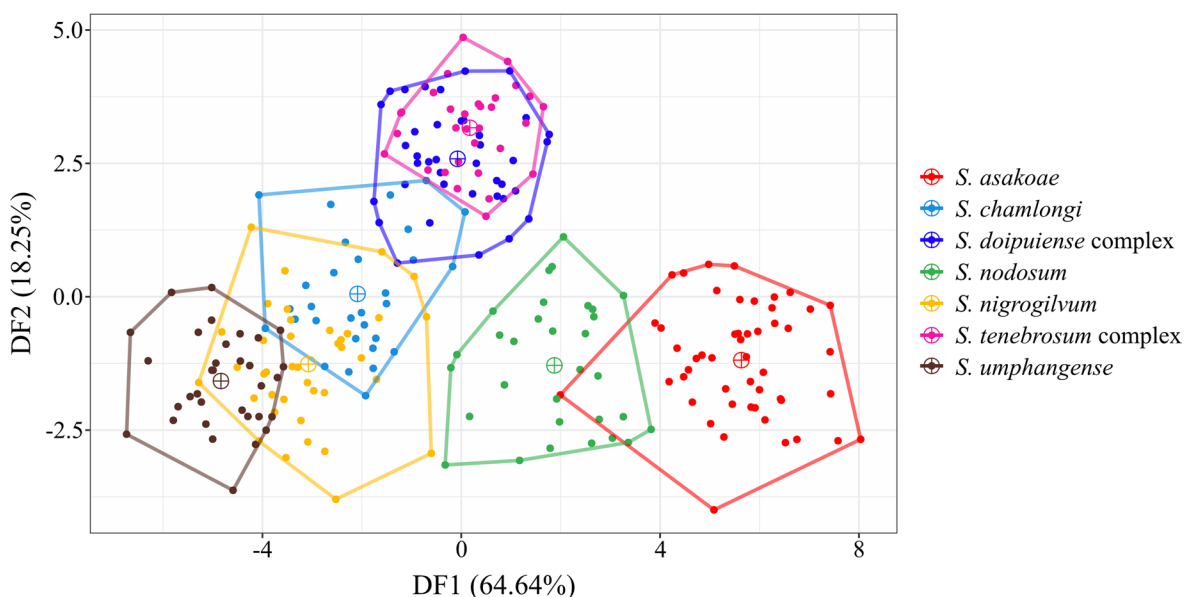

Fig. 5 Factor map based on discriminant analysis (DA) showing the shape divergence of seven black fly species. Each polygon represents a different species, with dots indicating individual specimens and a sun cross marking the mean values for each species

Table 3 Pairwise Mahalanobis distances and significant differences in wing shape of seven black fly species

Species	1	2	3	4	5	6	7
(1) *S. asakoae*	–						
(2) *S. chamlongi*	8.13[*]	–					
(3) *S. doipuiense* complex	7.03[*]	4.36[*]	–				
(4) *S. nodosum*	5.79[*]	6.13[*]	5.69[*]	–			
(5) *S. nigrogilvum*	8.86[*]	3.41[*]	5.13[*]	6.25[*]	–		
(6) *S. tenebrosum* complex	7.29[*]	4.77[*]	2.69[*]	5.65[*]	5.87[*]	–	
(7) *S. umphangense*	10.56[*]	4.24[*]	6.56[*]	7.68[*]	2.84[*]	7.11[*]	–

The superscript asterisks (*) after each Mahalanobis distance values denote statistically significant differences between black fly species at $p < 0.05$
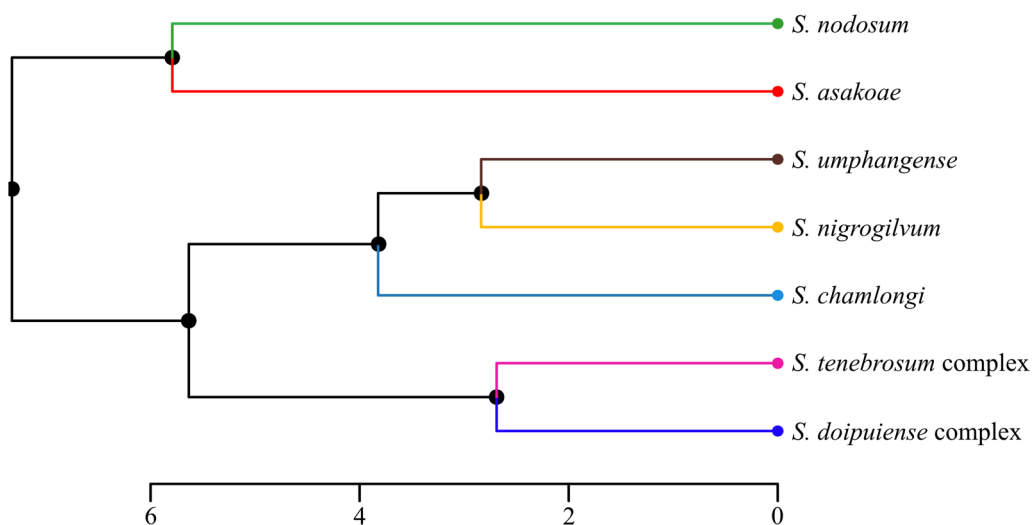
Aupalee *et al. Parasites & Vectors*   (2024) 17:508

Page 9 of 17

Fig. 6 UPGMA dendrogram based on the Mahalanobis distances between average group shapes showing the phenetic relationship of wing shape among seven black fly species. The scale bar represents the Mahalanobis distance

Table 4 Percentage of correct identification based on cross-validated classification of the wing size (centroid size) and wing shape (Mahalanobis distance values) of seven black fly species

Species	Percentage of correct classification (assigned/observed)	
	Based on wing size	Based on wing shape
S. asakoae	56.00% (28/50)	100.00% (50/50)
S. chamlongi	23.33% (7/30)	80.00% (24/30)
S. doipuiense complex	46.15% (18/39)	89.74% (35/39)
S. nodosum	29.03% (9/31)	96.77% (30/31)
S. nigrogilvum	41.03% (16/39)	76.92% (30/39)
S. tenebrosum complex	45.16% (14/31)	87.10% (27/31)
S. umphangense	84.85% (28/33)	84.85% (28/33)
Total performance	47.43% (120/253)	88.54% (224/253)

T = 0.379. An overlap between the maximum intraspecific and minimum interspecific divergences was also noted, suggesting the absence of a barcoding gap (Fig. 7).

The maximum intraspecific genetic distance based on the K2P model ranged from 0.15% (*S. chamlongi*) to 7.92% (*S. asakoae*). Most species showed low intraspecific divergences (maximum value < 3%). The exception was *S. asakoae*, which displayed the highest intraspecific divergence (maximum value > 7%) (Table 6).

The mean interspecific genetic divergences ranged from 2.64% (*S. tenebrosum* complex versus *S. doipuiense* complex) to 16.08% (*S. asakoae* versus *S. nodosum*), with the highest value of 17.13% (*S. asakoae* versus *S. chamlongi*). Low interspecific genetic divergence values were observed in two species pairs: *S. tenebrosum* complex

Table 5 Percentage of correctly assigned individuals based on the cross-validated classification of the wing shape of seven black fly species

Species	Classified as							Total	Correct identification
	1	2	3	4	5	6	7		
(1) *S. asakoae*	50	0	0	0	0	0	0	50	100.00%
(2) *S. chamlongi*	0	24	1	0	4	1	0	30	80.00%
(3) *S. doipuiense* complex	0	1	35	0	1	2	0	39	89.74%
(4) *S. nodosum*	0	1	0	30	0	0	0	31	96.77%
(5) *S. nigrogilvum*	0	4	1	0	30	0	4	39	76.92%
(6) *S. tenebrosum* complex	0	0	4	0	0	27	0	31	87.10%
(7) *S. umphangense*	0	0	0	0	5	0	28	33	84.85%
Correctly assigned/total individual								224/253	88.54%

The rows represent given species, while columns represent predicted species
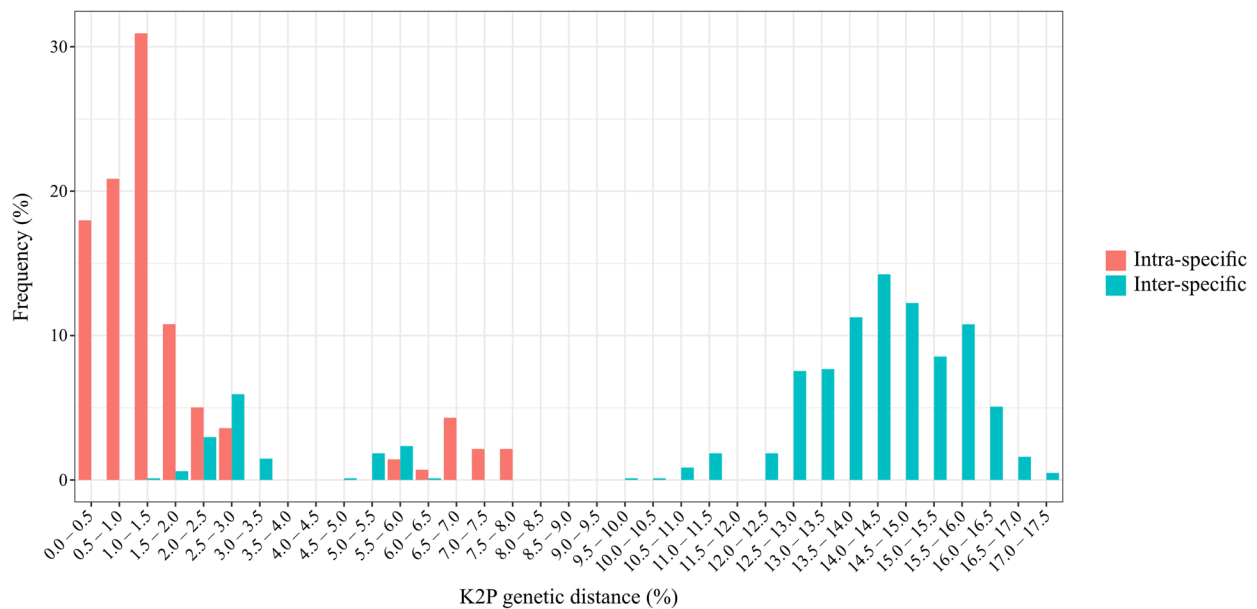
Fig. 7 Frequency distribution of intraspecific and interspecific K2P genetic distances based on the *COI* gene of seven human-biting black fly species

Table 6 Mean intraspecific (in bold) and interspecific genetic distances (%) with maximum values indicated in parentheses among seven human-biting black fly species

Species	1	2	3	4	5	6	7
(1) *S. asakoae*	**5.49 (7.92)**						
(2) *S. chamlongi*	15.69 (17.13)	**0.15 (0.15)**					
(3) *S. doipuiense* complex	14.97 (16.09)	13.01 (13.53)	**1.11 (1.86)**				
(4) *S. nodosum*	16.08 (17.00)	14.46 (14.79)	15.46 (16.14)	**0.23 (0.31)**			
(5) *S. nigrogilvum*	15.9 (17.07)	11.07 (11.38)	12.83 (13.75)	14.12 (14.42)	**0.73 (1.23)**		
(6) *S. tenebrosum* complex	14.91 (15.71)	13.22 (13.71)	2.64 (3.30)	14.61 (15.93)	13.21 (13.93)	**1.48 (2.81)**	
(7) *S. umphangense*	15.72 (16.48)	10.82 (11.24)	14.18 (14.89)	14.29 (14.67)	5.512 (6.06)	13.81 (14.11)	**0.58 (1.07)**

and *S. doipuiense* complex, and *S. nigrogilvum* and *S. umphangense*, with maximum values of 3.30% and 6.06%, respectively. Meanwhile the remaining species pairs showed very high levels of interspecific divergence, with maximum values exceeding 11% (Table 6).

Species determination through a BLAST search

Using a BLAST search, all haplotypes could be identified to the species level (Table S1). Four out of seven species, including *S. nodosum*, *S. tenebrosum* complex, *S. nigrogilvum*, and *S. umphangense* were correctly classified to their respective species or complex with high sequence similarity (98–100%). On the other hand, seven haplotypes of *S. asakoae* displayed the highest similarity (> 99%) with several different species of the *S. asakoae* species-group as follows: *S. nanthaburiense* (H1),

S. chaowaense (H4), *S. pitasawatae* (H5), *S. tamdaoense* (H6), and *S. asakoae* (H3, H7), whereby the H2 haplotype was identical to three different species, namely *S. asakoae*, *S. vinhphucense*, and *S. hongthaii*. *S. chamlongi* and *S. doipuiense* complex were also ambiguously assigned to the species level. One haplotype (H9) of *S. chamlongi* matched perfectly to *S. phuluense*, while the other (H8) was identical to both *S. phuluense* and *S. chamlongi*. Additionally, the majority of haplotypes (9/10) of the *S. doipuiense* complex showed the highest similarity (> 98%) to the *S. tenebrosum* complex, with only one (H14) being accurately identified as the *S. doipuiense* complex with a sequence similarity of 98.63%.

Aupalee *et al. Parasites & Vectors* (2024) 17:508

Page 11 of 17

Efficiency of the *COI* gene for species identification

Species identification based on the *COI* sequences demonstrated high success rate, with 98.57% (69/70) correct identification for both the BM and BCM methods. The only exception was the misidentification of one specimen (TN5) of *S. tenebrosum* complex as *S. doipuiense* complex.

Phylogenetic analysis

Both NJ and ML phylogenetic trees based on the *COI* sequences yielded similar tree topologies. Thus, only the ML tree is demonstrated (Fig. 8). Three species, namely *S. nigrogilvum*, *S. nodosum*, and *S. umphangense* were identified as distinct species, forming their own monophyletic groups with strong bootstrap support. In contrast, the remaining four species—*S. asakoae*, *S. tenebrosum* complex, *S. doipuiense* complex, and *S. chamlongi*—were not monophyletic. Sequences of *S. chamlongi* were clustered with *S. phuluense* from Vietnam, while the sequences of *S. tenebrosum* complex were intermixed with *S. doipuiense* complex. Notably, seven haplotypes of *S. asakoae* were divided into three subclades and placed into different species members of the *S. asakoae* species-group as follows: (1) *S. asakoae*/*S. vinhphucense*/*S. hongthaii* for H2, H3, and H7; (2) *S. pitasawatae* for H5; (3) *S. tamdaoense*/*S. myanmarense* for H6; (4) *S. nanthaburiense*/*S. monglaense* for H1; (5) *S. chaowaense* for H4.

Species delimitation analysis

Three species delimitation methods (ASAP, PTP, and GMYC) mostly supported seven morphospecies, as summarized in Fig. 9. Both ASAP and PTP methods identified eight putative species, while GMYC method
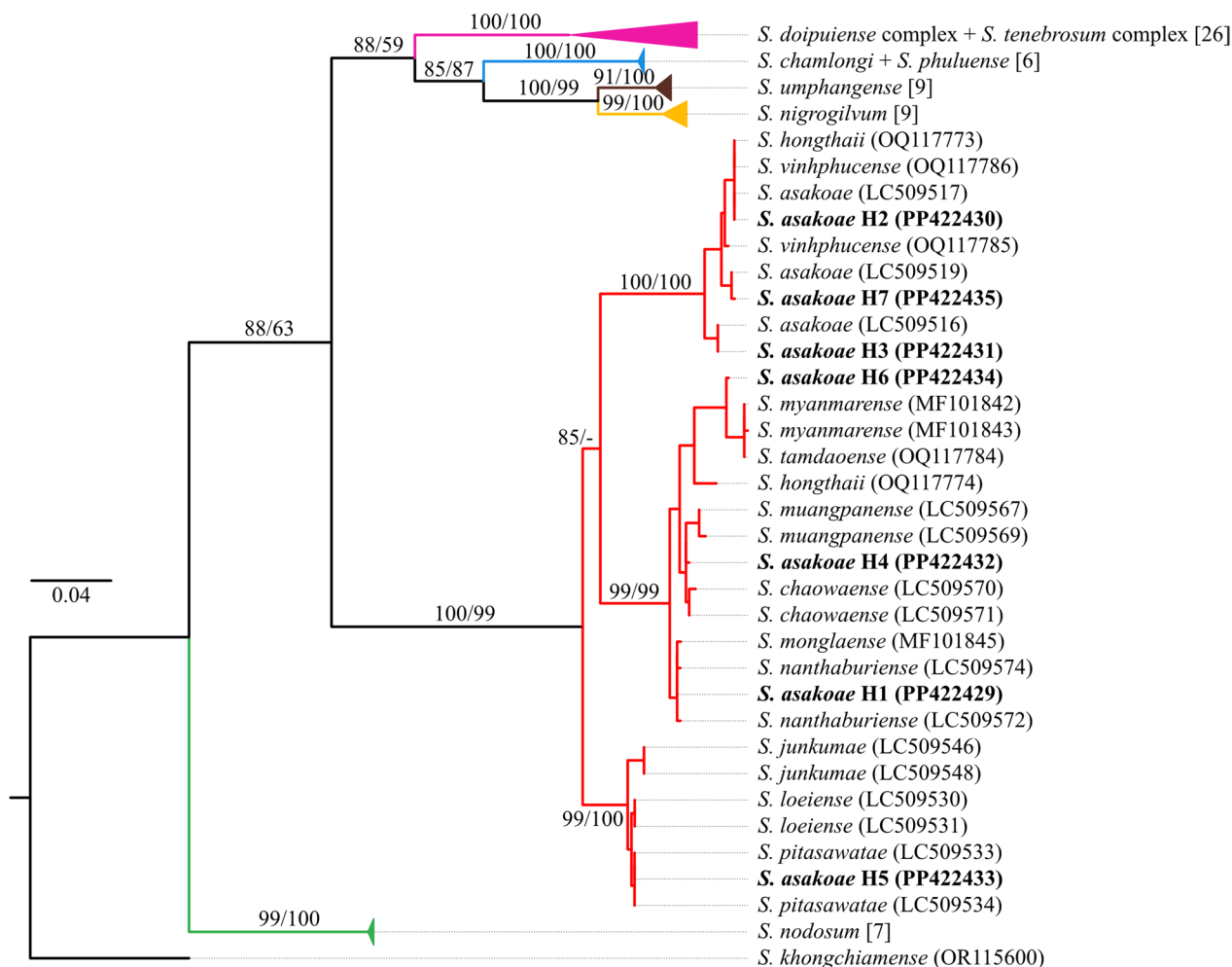

Fig. 8 Maximum likelihood phylogenetic tree based on 585 bp *COI* gene of seven human-biting black fly species and their related species. Bootstrap support values (ML/NJ) greater than 50% are indicated near the branches. Some distinct clades were collapsed for clearer presentation, and the number of sequences falling within those clades is indicated in square brackets. Sequences obtained in this study are highlighted in bold type. All sequences used for constructing the tree are detailed in Table S2
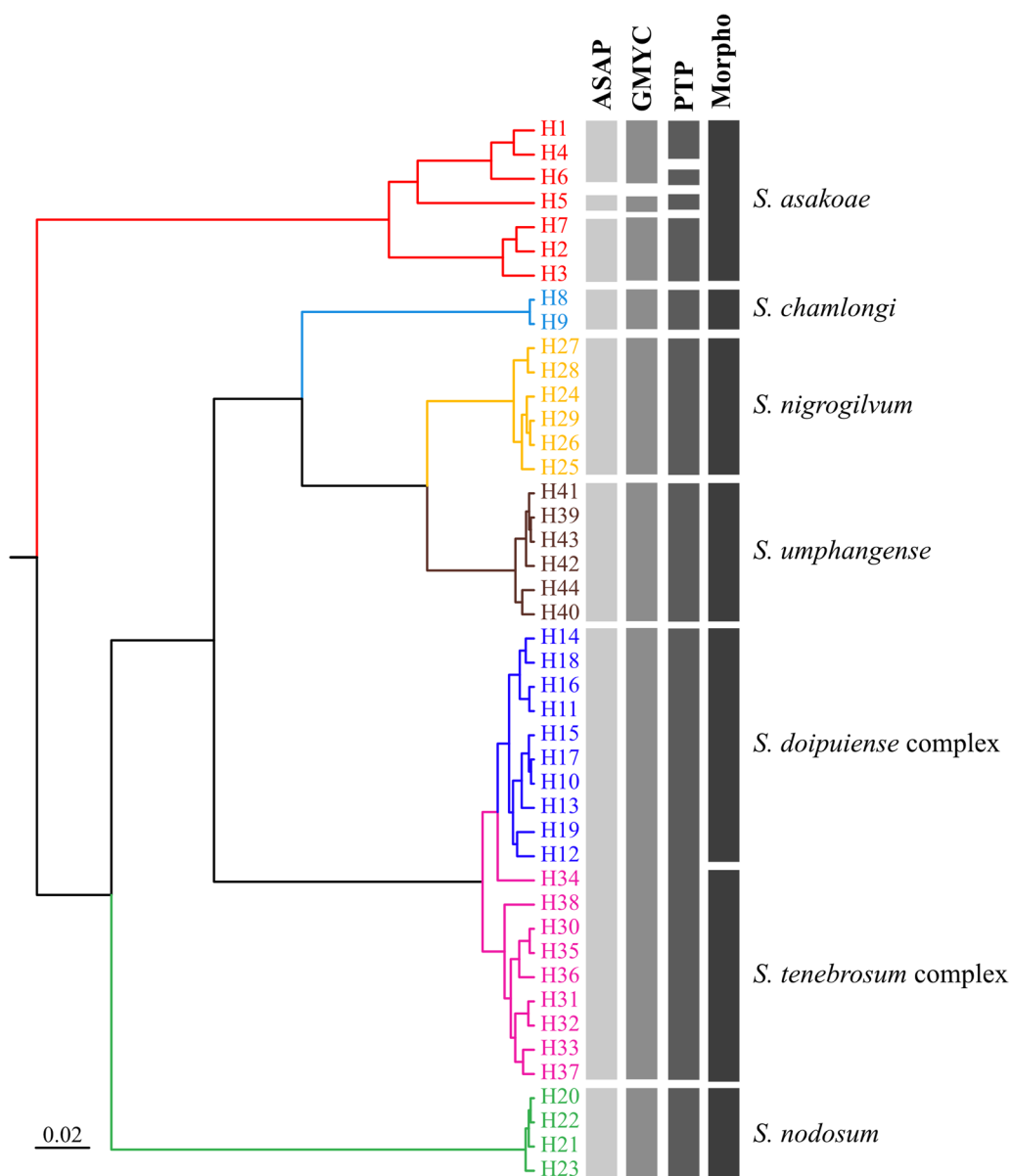
Fig. 9 Summary of the three species delimitation analyses (ASAP, GMYC, and PTP) based on the *COI* haplotypes from seven different nominal species of black flies. The maximum clade credibility tree built from BEAST is colored according to morphospecies. The vertical bars at the tips of the tree correspond to the result of each species delimitation method and morphological identification, respectively. Detailed information of each haplotype is provided in Table S2

recovered more putative species (nine species). All species delimitation methods merged *S. tenebrosum* complex and *S. doipuiense* complex into a single species, disagreeing with their morphologically defined species. Regarding *S. asakoae*, seven haplotypes were divided into three (ASAP and PTP) up to four (GMYC) putative species, suggesting cryptic diversity in this species.

Discussion

Here, we demonstrate for the first time that landmark-based GM of wing shape is a promising tool for the identification of the adult human-biting black flies in Thailand on a species level, although not with perfection. As expected, wing shape analysis is superior to wing size analysis in distinguishing black fly species, consistent with findings in numerous previous reports across various insect groups [46–48, 89, 90]. Unlike wing size,

Aupalee *et al. Parasites & Vectors*   (2024) 17:508

Page 13 of 17

which is susceptible to environmental influences and is not a suitable parameter for distinguishing species [57, 91], wing shape appears to be a fixed trait that preserves genetic information, making it a desirable species-specific indicator [92, 93]. Our allometric analysis also indicated that one variable (wing size) tends to increase, while the other (wing shape) tends to decrease (shows a negative correlation), as has been observed in several medically and forensically important insects, e.g., *Anopheles barbirostris* mosquitoes [46], *Armigeres* mosquitoes [50], *Culex vishnui* subgroup [94], and *Stomoxys* flies [90]. Therefore, this study excluded wing size data before wing shape analysis. Noticeably, our GM analysis based on wing shape was often unable to correctly assign the closely related species to their respective species. This result aligns with expectations, given the high morphological similarities between *S. umphangense* and *S. nigrogilvum*, where species separation relies mainly on subtle difference in the leg color of the fore tibia [14]. Similarly, the distinction of the two closely related species complexes, *S. tenebrosum* complex and *S. doipuiense* complex, is feasible based on certain features of the legs, specifically the coloration of the hind tibia and basitarsus [95].

The phenotypic relationships among seven black fly species mostly align with the phylogenetic tree based on the *COI* gene, suggesting that landmark-based GM analysis of wing shape could be used as an alternative tool for evolutionary studies, taxonomy, and systematics [51, 61, 94]. However, both phenotypic and phylogenetic analyses erroneously placed *S. nodosum* in the wrong group, contradicting its morphological classification and previous molecular studies [58, 96]. Instead of assigning all seven species to their respective subgenus, *S. nodosum* of the subgenus *Simulium* s.l. was placed in a distinct group or clustered as a sister species with *S. asakoae* of the subgenus *Gomphostilbia*. The incorrect assignment of *S. nodosum* seems to be due to the lack of intermediate taxa in the analyses. Therefore, incorporating additional black fly specimens of different species and subgenera into the analyses is recommended to improve both phenotypic and phylogenetic accuracy [97, 98].

In this study, we also assessed the performance of wing GM analysis in comparison to DNA barcoding based on the *COI* gene for distinguishing morphologically defined species. DNA barcoding clearly outperformed wing GM analysis, demonstrating an almost perfect efficiency (>98%) in species identification using both BM and BCM methods. The high accuracy (>90%) of DNA barcoding in distinguishing Thai black fly species was also observed in previous studies, even when analyzing a larger number of species (41–89 nominal species) [35, 96]. Further, our phylogenetic analysis of the *COI* gene coupled with

species delimitation analysis revealed hidden diversity within *S. asakoae*, suggesting the presence of up to four putative species. A previous molecular study using the *COI* gene also indicated that *S. asakoae* in Thailand consisted of at least seven groups [34]. Subsequent investigations, which extensively analyzed a large number of morphologically defined *S. asakoae* specimens further confirmed this observation, with a total of 23 new species described in recent years [99–101]. The high morphological variability and the high similarity of the *COI* sequences of several members of the *S. asakoae* species-group hampers the correct assignment of our *S. asakoae* specimens to the defined morphospecies [99, 102]. Initially, DNA barcoding was considered highly effective in distinguishing the true *S. asakoae* from other members in the *S. asakoae* species-group [102]. However, a recent study in Vietnam [39], as well as this study, demonstrated that the *COI* gene is no longer a suitable barcoding marker. In these studies, two related species from Vietnam, namely *S. hongthaii* and *S. vinhphucense*, were placed in the same clade as the true *S. asakoae*, leading to their delimitation as a single species. Some previous reports also suggested that the *COI* gene, or even the rapidly evolving nuclear *BZF* gene provide insufficient signal to distinguish most members of the *S. asakoae* species-group [35, 39, 99, 103]. To overcome this problem, further studies using more variable gene markers, such as the elongation complex protein 1 (*ECP1*), the 5-intron gene (*5intG*) [104], or molybdenum cofactor sulfurase (*MCS*) [105], are required to enhance species differentiation within the *S. asakoae* species-group. Additionally, we found that DNA barcoding was ineffective in identifying *S. tenebrosum* complex and *S. doipuiense* complex, and three species delimitation methods further supported this result by merging them as a single species [35, 39]. A more recent study examining the efficiency of two rapidly evolving nuclear genes suggested that the *ECP1* gene is a promising barcoding marker for the successful identification of the two species complexes [106]. The molecular analysis in this study also revealed a similar result that *S. chamlongi* is not monophyletic as its clade including *S. phuluense* from Vietnam [39]. It may be presumed that *S. chamlongi* and *S. phuluense* are morphologically distinct but molecularly homosequential, since they are readily distinguished by the color of female legs, the number of male upper-eye (large) facets and the presence or absence of tubercles on the pupal head [107, 108]. This suggests the need for additional genetic markers beyond the *COI* gene to resolve their phylogenetic relationships.

Although the accuracy of landmark-based GM of wing shape for black fly species identification in this study does not reach that of DNA barcoding, the results suggest that it is a promising complementary method to traditional

Aupalee *et al. Parasites & Vectors*   (2024) 17:508

Page 14 of 17

and molecular methods. In addition, wing GM analysis is simple, reliable, cost-effective, rapid, and only needs nondamaged wings, in contrast to molecular identification [47, 61, 109]. Since this is the first study that applies wing GM analysis for black fly species identification, we focus on the most important species (anthropophilic species) and use the most popular method, landmark-based GM [56, 57]. Further studies that include more species of different subgenera and employ both landmark- and outline-based GM approaches are needed to determine the extent to which wing GM analysis can serve as a tool for identifying adults of black fly species.

Conclusions

In this research, we demonstrate that landmark-based GM analysis of wing shape, which achieves greater accuracy than wing size analysis in species identification, is a promising, reliable tool for supplementing and enhancing morphological identification of black fly adults. Our molecular analysis suggests that there may be up to four putative species within the morphologically defined *S. asakoae*.

Abbreviations

ASAP   Assemble species by automatic partitioning
BCM   Best close match
BM   Best match
COI   Cytochrome *c* oxidase subunit I
GM   Geometric morphometrics
GMYC   Generalized mixed yule coalescent
PCR   Polymerase chain reaction
PTP   Poisson tree processes

Supplementary Information

The online version contains supplementary material available at https://doi.org/10.1186/s13071-024-06597-8.

Additional file 1: Table S1. Results from the NCBI BLAST search of black fly samples based on *COI* gene

Additional file 2: Table S2. Details of *COI* sequences generated from the present study and retrieved from NCBI GenBank databased used for molecular analysis

---

Author contributions
KA conceptualized the idea of the study, designed the experiments, performed laboratory investigations, analyzed the data and wrote the paper. KA and WS collected specimens. WS, KL, SS, HT, and AS gave advice and revised the paper. KA, KL, and AS interpreted the results. AS managed the project and provided resources.

Availability of data and materials
The authors confirm that all data supporting the findings of this study are available within the article. All sequences generated from the study have been deposited in the GenBank database with assigned accession numbers PP422429–PP422472.

Declarations

Ethics approval and consent to participate
The procedures and research methodology used in this study were approved by the Research Ethics Committee (Institutional Animal Care and Use Committee) (protocol number: 28/2564) of the Faculty of Medicine, Chiang Mai University, Chiang Mai Province, Thailand.

Consent for publication
All authors have read and approved the final version of the manuscript.

Competing interests
The authors declare no competing interests.

Author details
[1]Parasitology and Entomology Research Cluster (PERC), Department of Parasitology, Faculty of Medicine, Chiang Mai University, Chiang Mai 50200, Thailand. [2]Entomology Section, Queen Sirikit Botanic Garden, Mae Rim, Chiang Mai 50180, Thailand. [3]Tropical Infectious Diseases Research and Education Centre (TIDREC), Higher Institution Centre of Excellence (HICoE), Universiti Malaya, 50603 Kuala Lumpur, Malaysia.

References

1. Adler PH. World blackflies (Diptera: Simuliidae): a comprehensive revision of the taxonomic and geographical inventory [2024]. 2024. https://biomia.sites.clemson.edu/pdfs/blackflyinventory.pdf.
2. Orange JS, Song LA, Twarog FJ, Schneider LC. A patient with severe black fly (Simuliidae) hypersensitivity referred for evaluation of suspected immunodeficiency. Ann Allergy Asthma Immunol. 2004;92:276–80.
3. Hellberg W, Mellor PS, Torsteinsdottir S, Marti E. Insect bite hypersensitivity in the horse: comparison of IgE-binding proteins in salivary gland extracts from *Simulium vittatum* and *Culicoides nubeculosus*. Vet Immunol Immunopathol. 2009;132:62–7.
4. Schaffartzik A, Weichel M, Crameri R, Bjornsdottir TS, Prisi C, Rhyner C, et al. Cloning of IgE-binding proteins from *Simulium vittatum* and their potential significance as allergens for equine insect bite hypersensitivity. Vet Immunol Immunopathol. 2009;132:68–77.
5. Schaffartzik A, Marti E, Crameri R, Rhyner C. Cloning, production and characterization of antigen 5 like proteins from *Simulium vittatum* and *Culicoides nubeculosus*, the first cross-reactive allergen associated with equine insect bite hypersensitivity. Vet Immunol Immunopathol. 2010;137:76–83.
6. Schaffartzik A, Hamza E, Janda J, Crameri R, Marti E, Rhyner C. Equine insect bite hypersensitivity: what do we know? Vet Immunol Immunopathol. 2012;147:113–26.
7. Chattopadhyay P, Goyary D, Dhiman S, Rabha B, Hazarika S, Veer V. Immunomodulating effects and hypersensitivity reactions caused by Northeast Indian black fly salivary gland extract. J Immunotoxicol. 2014;11:126–32.
8. Chiriac A, Brzezinski P, Miron L, Moldovan C, Podoleanu C, Stolnicu S. Simuliosis–a dermatosis caused by black flies. Allergol Int. 2016;65:217–8.
9. Adler PH, McCreadie JW. Black flies (Simuliidae). In: Mullen GR, Durden LA, editors. Medical and veterinary entomology. 3rd ed. London: Academic Press; 2019. p. 237–59.
10. Basanez MG, Boussinesq M. Population biology of human onchocerciasis. Philos Trans R Soc Lond B Biol Sci. 1999;354:809–26.

Aupalee *et al. Parasites & Vectors*   (2024) 17:508

Page 15 of 17

11. World Health Organization, Department of Neglected Tropical Disease. Ending the neglect to attain the sustainable development goals: a road map for neglected tropical diseases 2021–2030. 2020. https://iris.who.int/bitstream/handle/10665/338565/9789240010352-eng.pdf?sequence=1

12. Choochote W, Takaoka H, Fukuda M, Otsuka Y, Aoki C, Eshima N. Seasonal abundance and daily flying activity of black flies (Diptera: Simuliidae) attracted to human baits in Doi Inthanon National Park, northern Thailand. Med Entomol Zool. 2005;56:335–48.

13. Pramual P, Thaijarern J, Wongpakam K. DNA barcoding of human-biting black flies (Diptera: Simuliidae) in Thailand. Acta Trop. 2016;164:33–40.

14. Takaoka H, Srisuka W, Saeung A. A new human-biting black fly species of *Simulium* (*Simulium*) (Diptera: Simuliidae) from Thailand. J Med Entomol. 2017;54:945–8.

15. Srisuka W, Takaoka H, Taai K, Maleewong W, Aupalee K, Saeung A. Morphological description and genetic analysis of a new black fly species (Diptera: Simuliidae) in the subgenus *Asiosimulium* from central Thailand. Parasit Vectors. 2024;17:379.

16. Gomontean B, Jumpato W, Wongpakam K, Tangkawanit U, Wannasingha W, Thanee I, et al. Diversity, distribution and host blood meal analysis of adult black flies (Diptera: Simuliidae) from Thailand. Insects. 2024;15:74.

17. Aupalee K, Saeung A, Srisuka W, Fukuda M, Streit A, Takaoka H. Seasonal filarial infections and their black fly vectors in Chiang Mai province, northern Thailand. Pathogens. 2020;9:512.

18. Fukuda M, Choochote WET, Bain O, Aoki C, Takaoka H. Natural infections with filarial larvae in two species of black flies (Diptera: Simuliidae) in northern Thailand. Jpn J Trop Med Hyg. 2003;31:99–102.

19. Takaoka H, Choochote W, Aoki C, Fukuda M, Bain O. Black flies (Diptera: Simuliidae) attracted to humans and water buffalos and natural infections with filarial larvae, probably *Onchocerca* sp., in northern Thailand. Parasite. 2003;10:3–8.

20. Ishii Y, Choochote W, Bain O, Fukuda M, Otsuka Y, Takaoka H. Seasonal and diurnal biting activities and zoonotic filarial infections of two *Simulium* species (Diptera: Simuliidae) in northern Thailand. Parasite. 2008;15:121–9.

21. Saeung A, Srisuka W, Aupalee K, Fukuda M, Otsuka Y, Taai K, et al. Natural infections with larvae of *Onchocerca* species type I in the human-biting black fly, *Simulium nigrogilvum* (Diptera: Simuliidae), in western Thailand. Acta Trop. 2020;204:105344.

22. Huang F, Srisuka W, Aupalee K, Streit A, Fukuda M, Pitasawat B, et al. Diversity of nematodes infecting the human-biting black fly species, *Simulium nigrogilvum* (Diptera: Simuliidae) in central Thailand. Acta Trop. 2021;224:106140.

23. Jumpato W, Tangkawanit U, Wongpakam K, Pramual P. Molecular detection of *Leucocytozoon* (Apicomplexa: Haemosporida) in black flies (Diptera: Simuliidae) from Thailand. Acta Trop. 2019;190:228–34.

24. Thaijarern J, Tangkawanit U, Wongpakam K, Pramual P. Molecular detection of *Trypanosoma* (Kinetoplastida: Trypanosomatidae) in black flies (Diptera: Simuliidae) from Thailand. Acta Trop. 2019;200:105196.

25. Pramual P, Thaijarern J, Tangkawanit U, Wongpakam K. Molecular identification of blood meal sources in black flies (Diptera: Simuliidae) suspected as *Leucocytozoon* vectors. Acta Trop. 2020;205:105383.

26. Stangarm J, Mintara R, Jumpato W, Gomontean B, Thanee I, Wongpakam K, et al. Molecular detection of blood protozoa and identification of black flies of the *Simulium varicorne* species group (Diptera: Simuliidae) in Thailand. Acta Trop. 2024;254:107207.

27. Yssouf A, Almeras L, Raoult D, Parola P. Emerging tools for identification of arthropod vectors. Future Microbiol. 2016;11:549–66.

28. Rivera J, Currie DC. Identification of Nearctic black flies using DNA barcodes (Diptera: Simuliidae). Mol Ecol Resour. 2009;9:224–36.

29. Adler PH, Huang S. Chromosomes as Barcodes: Discovery of a new species of black fly (Diptera: Simuliidae) from California, USA. Insects. 2022;13:903.

30. Thapa S, Adler PH, Chhetri S, Varma R, Henry W. Chromosomal evidence for a new cryptic species of black fly in the *Simulium praelargum* complex (Diptera: Simuliidae) from West Bengal, India. Zootaxa. 2017;4244:137–44.

31. Nascimento J, Hamada N, Andrade-Souza V, Adler PH. A new anthropophilic species of *Simulium* (*Trichodagmia*) (Diptera: Simuliidae) from

32. Adler PH, Fukuda M, Takaoka H, Reeves WK, Kim SK, Otsuka Y. Revision of *Simulium rufibasis* (Diptera: Simuliidae) in Japan and Korea: Chromosomes, DNA, and Morphology. J Med Entomol. 2020;57:388–403.

33. Hernandez-Triana LM, Montes De Oca F, Prosser SW, Hebert PD, Gregory TR, McMurtrie S. DNA barcoding as an aid for species identification in austral black flies (Insecta: Diptera: Simuliidae). Genome. 2017;60:348–57.

34. Jomkumsing P, Tangkawanit U, Wongpakam K, Pramual P. Who is biting you? DNA barcodes reveal cryptic diversity in human-biting black flies (Diptera: Simuliidae). Acta Trop. 2019;196:22–9.

35. Pramual P, Jomkumsing P, Wongpakam K, Wongwian P. DNA barcoding of tropical black flies (Diptera: Simuliidae) in Thailand: one decade of progress. Acta Trop. 2021;224:106116.

36. Hew YX, Ya'cob Z, Adler PH, Chen CD, Lau KW, Sofian-Azirun M, et al. DNA barcoding of black flies (Diptera: Simuliidae) in Indonesia. Parasit Vectors. 2023;16:248.

37. Izwan-Anas N, Low VL, Ya'cob Z, Lourdes EY, Halim MRA, Sofian-Azirun M, et al. DNA barcodes and species boundaries of black flies (Diptera: Simuliidae) in Malaysia. Arthropod Syst Phylogeny. 2023;81:931–43.

38. Kúdelová T, Krčmárik S, Lužáková I, Bujačková B, Matická K, Kúdela M. DNA barcoding of black flies (Diptera: Simuliidae) in Slovakia and its utility for species identification. Diversity. 2023;15:661.

39. Putt QY, Ya'cob Z, Adler PH, Chen CD, Hew YX, Izwan-Anas N, et al. From bites to barcodes: uncovering the hidden diversity of black flies (Diptera: Simuliidae) in Vietnam. Parasit Vectors. 2023;16:266.

40. Garros C, Dujardin J-P. Genetic and phenetic approaches to *Anopheles* systematics. London: InTech; 2013.

41. Sumruayphol S, Apiwathnasorn C, Ruangsittichai J, Sriwichai P, Attrapadung S, Samung Y, et al. DNA barcoding and wing morphometrics to distinguish three *Aedes* vectors in Thailand. Acta Trop. 2016;159:1–10.

42. Jaramillo ON, Dujardin JP, Calle-Londono D, Fonseca-Gonzalez I. Geometric morphometrics for the taxonomy of 11 species of *Anopheles* (*Nyssorhynchus*) mosquitoes. Med Vet Entomol. 2015;29:26–36.

43. Sontigun N, Samerjai C, Sukontason K, Wannasan A, Amendt J, Tomberlin JK, et al. Wing morphometric analysis of forensically important flesh flies (Diptera: Sarcophagidae) in Thailand. Acta Trop. 2019;190:312–9.

44. Champakaew D, Junkum A, Sontigun N, Sanit S, Limsopatham K, Saeung A, et al. Geometric morphometric wing analysis as a tool to discriminate female mosquitoes from different suburban areas of Chiang Mai province. Thailand PloS one. 2021;16:e0260333.

45. Limsopatham K, Klong-Klaew T, Fufuang N, Sanit S, Sukontason KL, Sukontason K, et al. Wing morphometrics of medically and forensically important muscid flies (Diptera: Muscidae). Acta Trop. 2021;222:106062.

46. Chaiphongpachara T, Changbunjong T, Laojun S, Sumruayphol S, Suwandittakul N, Kuntawong K, et al. Geometric morphometric and molecular techniques for discriminating among three cryptic species of the *Anopheles barbirostris* complex (diptera: culicidae) in Thailand. Heliyon. 2022;8:e11261.

47. Hadj-Henni L, Millot C, Lehrter V, Augot D. Wing morphometrics of biting midges (Diptera: Culicoides) of veterinary importance in Madagascar. Infect Genet Evol. 2023;114:105494.

48. Ardkhongharn N, Ravichotikul R, Aksornchai P, Weluwanarak T, Chaiphongpachara T, Changbunjong T. Wing geometric morphometrics to distinguish and identify *Haematobosca* flies (Diptera: Muscidae) from Thailand. Int J Parasitol Parasites Wildl. 2023;21:74–82.

49. Laojun S, Changbunjong T, Sumruayphol S, Chaiphongpachara T. Outline-based geometric morphometrics: wing cell differences for mosquito vector classification in the Tanaosri mountain range, Thailand. Acta Trop. 2024;250:107093.

50. Laojun S, Changbunjong T, Sumruayphol S, Pimsuka S, Chaiphongpachara T. Wing geometric morphometrics and DNA barcoding to distinguish three closely related species of *Armigeres* mosquitoes (Diptera: Culicidae) in Thailand. Vet Parasitol. 2024;325:110092.

51. Pepinelli M, Spironello M, Currie DC. Geometric morphometrics as a tool for interpreting evolutionary transitions in the black fly wing (Diptera: Simuliidae). Zool J Linn Soc. 2013;169:377–88.

52. Gérard M, Martinet B, Dehon M, Rasmont P, Williams PH, Michez D. The utility of wing morphometrics for assigning type specimens to cryptic bumblebee species. Syst Entomol. 2020;45:849–56.

Aupalee *et al. Parasites & Vectors*   (2024) 17:508

Page 16 of 17

53. Boumaza M, Merabti B, Adjami Y, Ouakid ML, Carvajal TM. Geometric morphometric wing analysis of avian malaria vector, *Culiseta longiareo-lata*, from two locations in Algeria. Insects. 2022;13:1031.

54. Chaiphongpachara T, Duvallet G, Changbunjong T. Wing phenotypic variation among *Stomoxys calcitrans* (Diptera: Muscidae) populations in Thailand. Insects. 2022;13:405.

55. Santoni MM, Magri LA, de Oliveira SV, da Silva BH, Del Lama MA. Sex ratio, sexual eimorphism, and wing geometric morphometrics in species of *Trypoxylon* Latreille, 1796 (Hymenoptera: Crabronidae). Neotrop Entomol. 2023;52:1005–17.

56. Dujardin J-P. Morphometrics applied to medical entomology. Infect Genet Evol. 2008;8:875–90.

57. Lorenz C, Almeida F, Almeida-Lopes F, Louise C, Pereira SN, Petersen V, et al. Geometric morphometrics in mosquitoes: what has been measured? Infect Genet Evol. 2017;54:205–15.

58. Takaoka H, Srisuka W, Saeung A. Checklist and keys for the black flies (Diptera: Simuliidae) of Thailand. Med Entomol Zool. 2019;70:53–77.

59. Arnqvist G, Martensson T. Measurement error in geometric morphometrics: empirical strategies to assess and reduce its impact on measures of shape. Acta Zool Acad Sci Hung. 1998;44:73–96.

60. Gidaszewski NA, Baylac M, Klingenberg CP. Evolution of sexual dimorphism of wing shape in the *Drosophila melanogaster* subgroup. BMC Evol Biol. 2009;9:110.

61. Sontigun N, Sukontason KL, Zajac BK, Zehner R, Sukontason K, Wannasan A, et al. Wing morphometrics as a tool in species identification of forensically important blow flies of Thailand. Parasit Vectors. 2017;10:229.

62. Bookstein FL. Morphometric tools for landmark data: geometry and biology. New York: Cambridge University Press; 1991.

63. Gower JC. Generalized procrustes analysis. Psychometrika. 1975;40:33–51.

64. Rohlf FJ. Rotational fit (Procrustes) methods. In: Rohlf F, Bookstein F, (eds). Proceedings of the Michigan Morphometrics Workshop Special Pu Ann Arbor. The University of Michigan Museum of Zoology. 1990. p. 227–36.

65. Murtagh F, Contreras P. Algorithms for hierarchical clustering: an overview, II. WIREs Data Min Knowl Discovery. 2017;7:e1219.

66. Manly BFJ. Multivariate statistical methods: a primer. 3rd ed. USA: Chapman and Hall/CRC; 2004.

67. Dujardin J-P, Dujardin S, Kaba D, Santill An-Guayasamín S, Villacís AG, Piyaselakul S, et al. The maximum likelihood identification method applied to insect morphometric data. Zool Syst. 2017;42:46–58.

68. Mahalanobis PC. On the generalized distance in statistics. Proc Natl Inst Sci (Calcutta). 1936;2:49–55.

69. Dujardin S, Dujardin J-P. Geometric morphometrics in the cloud. Infect Genet Evol. 2019;70:189–96.

70. Team R: RStudio: integrated development for R. Boston, MA; 2020.

71. Folmer O, Black M, Hoeh W, Lutz R, Vrijenhoek R. DNA primers for amplification of mitochondrial cytochrome c oxidase subunit I from diverse metazoan invertebrates. Mol Mar Biol Biotechnol. 1994;3:294–9.

72. Kearse M, Moir R, Wilson A, Stones-Havas S, Cheung M, Sturrock S, et al. Geneious basic: an integrated and extendable desktop software platform for the organization and analysis of sequence data. Bioinformatics. 2012;28:1647–9.

73. Kimura M. A simple method for estimating evolutionary rates of base substitutions through comparative studies of nucleotide sequences. J Mol Evol. 1980;16:111–20.

74. Stecher G, Tamura K, Kumar S. Molecular evolutionary genetics analysis (MEGA) for macOS. Mol Biol Evol. 2020;37:1237–9.

75. Tamura K, Stecher G, Kumar S. MEGA11: molecular evolutionary genetics analysis version 11. Mol Biol Evol. 2021;38:3022–7.

76. Meier R, Shiyang K, Vaidya G, Ng PK. DNA barcoding and taxonomy in Diptera: a tale of high intraspecific variability and low identification success. Syst Biol. 2006;55:715–28.

77. Edgar RC. MUSCLE: multiple sequence alignment with high accuracy and high throughput. Nucleic Acids Res. 2004;32:1792–7.

78. Saitou N, Nei M. The neighbor-joining method: a new method for reconstructing phylogenetic trees. Mol Biol Evol. 1987;4:406–25.

79. Nguyen LT, Schmidt HA, von Haeseler A, Minh BQ. IQ-TREE: a fast and effective stochastic algorithm for estimating maximum-likelihood phylogenies. Mol Biol Evol. 2015;32:268–74.

80. Hoang DT, Chernomor O, von Haeseler A, Minh BQ, Vinh LS. UFBoot2: improving the ultrafast bootstrap approximation. Mol Biol Evol. 2018;35:518–22.

81. Kalyaanamoorthy S, Minh BQ, Wong TKF, von Haeseler A, Jermiin LS. ModelFinder: fast model selection for accurate phylogenetic estimates. Nat Methods. 2017;14:587–9.

82. Puillandre N, Brouillet S, Achaz G. ASAP: assemble species by automatic partitioning. Mol Ecol Resour. 2021;21:609–20.

83. Zhang J, Kapli P, Pavlidis P, Stamatakis A. A general species delimitation method with applications to phylogenetic placements. Bioinformatics. 2013;29:2869–76.

84. Pons J, Barraclough TG, Gomez-Zurita J, Cardoso A, Duran DP, Hazell S, et al. Sequence-based species delimitation for the DNA taxonomy of undescribed insects. Syst Biol. 2006;55:595–609.

85. Drummond AJ, Suchard MA, Xie D, Rambaut A. Bayesian phylogenetics with BEAUti and the BEAST 1.7. Mol Biol Evol. 2012;29:1969–73.

86. Darriba D, Taboada GL, Doallo R, Posada D. jModelTest 2: more models, new heuristics and parallel computing. Nat Methods. 2012;9:772.

87. Drummond AJ, Rambaut A. BEAST: Bayesian evolutionary analysis by sampling trees. BMC Evol Biol. 2007;7:214.

88. Ezard T, Fujisawa T, Barraclough T. splits: SPecies' LImits by Threshold Statistics. R package version 1.0–14/r31. 2009.

89. Changbunjong T, Prakaikowit N, Maneephan P, Kaewwiset T, Weluwanarak T, Chaiphongpachara T, et al. Landmark data to distinguish and identify morphologically close *Tabanus* spp. (Diptera: Tabanidae). Insects. 2021;12:974.

90. Changbunjong T, Chaiphongpachara T, Weluwanarak T. Species discrimination of Stomoxys flies *S. bengalensis*, *S. calcitrans*, and *S. sitiens* (Diptera: Muscidae) using wing geometric morphometrics. Animals. 2023;13:647.

91. Gomez GF, Marquez EJ, Gutierrez LA, Conn JE, Correa MM. Geometric morphometric analysis of Colombian *Anopheles albimanus* (Diptera: Culicidae) reveals significant effect of environmental factors on wing traits and presence of a metapopulation. Acta Trop. 2014;135:75–85.

92. Lorenz C, Suesdek L. The use of wing shape for characterising macroevolution in mosquitoes (Diptera: Culicidae). Infect Genet Evol. 2020;77:104052.

93. Chonephetsarath S, Raksakoon C, Sumruayphol S, Dujardin JP, Potiwat R. The unequal taxonomic signal of mosquito wing cells. Insects. 2021;12:376.

94. Saiwichai T, Laojun S, Chaiphongpachara T, Sumruayphol S. Species identification of the major Japanese Encephalitis vectors within the *Culex vishnui* Subgroup (Diptera: Culicidae) in Thailand using geometric morphometrics and DNA barcoding. Insects. 2023;14:131.

95. Takaoka H, Srisuka W, Low VL, Saeung A. Morphological and molecular analyses of *Simulium rufibasis* (Diptera: Simuliidae) in Thailand. J Med Entomol. 2019;56:408–15.

96. Pramual P, Adler PH. DNA barcoding of tropical black flies (Diptera: Simuliidae) of Thailand. Mol Ecol Resour. 2014;14:262–71.

97. Pollock DD, Zwickl DJ, McGuire JA, Hillis DM. Increased taxon sampling is advantageous for phylogenetic inference. Syst Biol. 2002;51:664–71.

98. Dong Z, Qu S, Landrein S, Yu WB, Xin J, Zhao W, et al. Increasing taxa sampling provides new insights on the phylogenetic relationship between *Eriobotrya* and *Rhaphiolepis*. Front Genet. 2022;13:831206.

99. Takaoka H, Srisuka W, Fukuda M, Saeung A. Twenty-one new species of the *Simulium* (*Gomphostilbia*) *asakoae* species group (Diptera, Simuliidae) in Thailand, with their genetic relationships. Zookeys. 2020;950:51–152.

100. Srisuka W, Aupalee K, Low VL, Yacob Z, Fukuda M, Saeung A, et al. A new species of *Simulium* (*Gomphostilbia*) (Diptera: Simuliidae) from Northern Thailand, with its genetic relationship in the *S. asakoae* species-group. Acta Trop. 2021;218:105889.

101. Srisuka W, Aupalee K, Fukuda M, Saeung A, Takaoka H. Morphological description and phylogenetic position of a new cryptic species in the *Simulium asakoae* species-group, *Simulium* (*Gomphostilbia*) *mokroense*, from Western Thailand. Acta Trop. 2022;228:106313.

102. Low VL, Srisuka W, Saeung A, Tan TK, Ya'cob Z, Yeong YS, et al. DNA barcoding of *Simulium asakoae* (Diptera: Simuliidae) from northern Thailand. J Med Entomol. 2020;57:1675–8.

103. Low VL, Takaoka H, Adler PH, Ya'cob Z, Norma-Rashid Y, Chen CD, et al. A multi-locus approach resolves the phylogenetic relationships of

Aupalee *et al. Parasites & Vectors*   *(2024) 17:508*

Page 17 of 17

the *Simulium asakoae* and *Simulium ceylonicum* species groups in Malaysia: evidence for distinct evolutionary lineages. Med Vet Entomol. 2015;29:330–7.

104. Senatore GL, Alexander EA, Adler PH, Moulton JK. Molecular systematics of the *Simulium jenningsi* species group (Diptera: Simuliidae), with three new fast-evolving nuclear genes for phylogenetic inference. Mol Phylogenet Evol. 2014;75:138–48.

105. Winkler IS, Blaschke JD, Davis DJ, Stireman JO 3rd, O'Hara JE, Cerretti P, et al. Explosive radiation or uninformative genes? origin and early diversification of tachinid flies (Diptera: Tachinidae). Mol Phylogenet Evol. 2015;88:38–54.

106. Pramual P, Jumpato W, Adler PH. Fast-evolving nuclear genes as barcoding markers for black flies (Diptera: Simuliidae) in Thailand. Acta Trop. 2023;246:106988.

107. Takaoka H, Sofian-Azirun M, Ya'cob Z, Chen CD, Lau KW, Low VL, et al. The black flies (Diptera: Simuliidae) of Vietnam. Zootaxa. 2017;4261:1–165.

108. Takaoka H, Suzuki H. The blackflies (Diptera: Simuliidae) from Thailand. Med Entomol Zool. 1984;35:7–45.

109. Sauer FG, Pfitzner WP, Jost H, Rauhoft L, Kliemke K, Lange U, et al. Using geometric wing morphometrics to distinguish *Aedes japonicus japonicus* and *Aedes koreicus*. Parasit Vectors. 2023;16:418.

Publisher's Note